Available online at www.sciencedirect.com
SCIENCE DIRECT
Journal of Magnetic Resonance 178 (2006) 1–10
JMR Journal of Magnetic Resonance
www.elsevier.com/locate/jmr

NMR determination of photorespiration in intact leaves using in vivo $^{13}CO_2$ labeling ☆

Lynette Cegelski, Jacob Schaefer *

Department of Chemistry, Washington University, St. Louis, MO 63130, USA

Received 26 August 2005; revised 3 October 2005
Available online 10 November 2005

Abstract

Solid-state ^{13}C NMR measurements of intact soybean leaves labeled by $^{13}CO_2$ lead to the conclusion that photorespiration is 17% of photosynthesis for a well-watered and fertilized plant. This is the first direct assessment of the level of photorespiration in a functioning plant. A $^{13}C\{^{31}P\}$ rotational-echo double-resonance (REDOR) measurement tracked the incorporation of ^{13}C label into intermediates in the Calvin cycle as a function of time. For labeling times of 5 min or less, the isotopic enrichment of the Calvin cycle depends on the flux of labeled carbon from $^{13}CO_2$, relative to the flux of unlabeled carbon from glycerate returned from the photorespiratory cycle. Comparisons of these two rates for a fixed value of the $^{13}CO_2$ concentration indicate that the ratio of the rate of photosynthesis to the rate of photorespiration of ribulose-1,5-bisphosphate carboxylase/oxygenase (Rubisco) in soybean leaves is 5.7. This translates into a photorespiratory CO_2 loss that is 21% of net CO_2 assimilation, about 80% of the value estimated from Rubisco kinetics parameters. The ratio of rates is reduced at low external CO_2 concentrations, as measured by net carbon assimilation rates. The carbon assimilation was determined from ^{13}C-label spin counts converted into total carbon by the REDOR-determined isotopic enrichments of the Calvin cycle. The net carbon assimilation rates indicate that the rate of decarboxylation of glycine is not directly proportional to the oxygenase activity of Rubisco as is commonly assumed.

Keywords: Carboxylase; Dipolar coupling; Magic-angle spinning; Oxygenase; Photorespiration; Photosynthesis; Solid-state NMR; Soybeans

1. Introduction

1.1. Photosynthesis and photorespiration

Rubisco[1] (ribulose-1,5-bisphosphate carboxylase/oxygenase) originally fixed carbon in an atmosphere of high CO_2 concentration and negligible O_2 concentration more than two billion years ago [1]. This carboxylase activity, termed photosynthesis, converts atmospheric CO_2 into carbon-rich compounds and leads to the release of O_2. When plants appeared on Earth, the oxygen content of the atmosphere increased. Rubisco now operates under a CO_2 concentration of about 380 ppm (by volume) and an O_2 concentration of 21% (210,000 ppm).

Photorespiration refers to the oxygenation of ribulose-1,5-bisphosphate (RuBP) by Rubisco and the events that are stimulated by the immediate production and subsequent rescue of a two-carbon molecule that is not compatible with the Calvin cycle. Carbon salvage requires machinery distributed over three organelles to convert a two-carbon molecule (glycolate) into a useful carbon source (glycerate) via the condensation of two glycines to form a serine with the concomitant release of CO_2 (Fig. 1). This process is known as the photorespiratory C_2 cycle. Photorespiration is generally considered a wasteful process, a side-reaction of Rubisco which Nature has been unable to avoid [2], although protection of

☆ This paper is based on work supported by the National Science Foundation under Grant No. MCB-0089905.
* Corresponding author. Fax: +1 314 935 4481.
E-mail address: jschaefer@wustl.edu (J. Schaefer).
[1] *Abbreviations used:* CPMAS, cross-polarization magic-angle spinning; REDOR, rotational-echo double resonance; RuBP, ribulose-1,5-bisphosphate; Rubisco, ribulose-1,5-bisphosphate carboxylase/oxygenase.

1090-7807/$ - see front matter © 2005 Elsevier Inc. All rights reserved.
doi:10.1016/j.jmr.2005.10.010

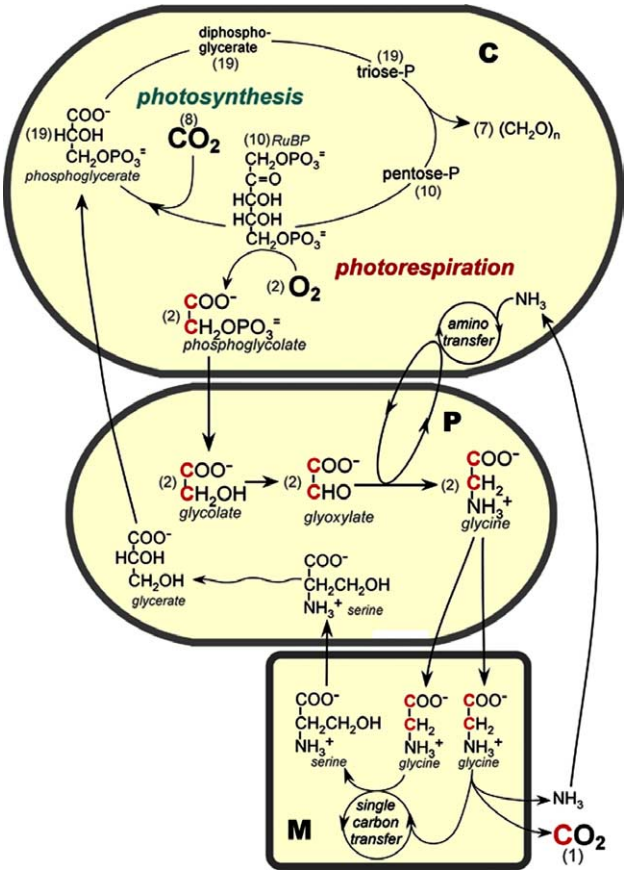

Fig. 1. The photorespiratory pathway (adapted from Ogren [6]). Oxygenation of ribulose bisphosphate (RuBP) leads to the production of the 2-carbon phosphoglycolate (red), which is partially recycled by serine synthesis leading to glycerate. This process requires machinery distributed over three organelles: the chloroplast (C), the peroxisome (P), and the mitochondrion (M). Concurrent energy balance processes via NAD/NADH and ATP/ADP conversions are omitted. The numbers in parentheses indicate stoichiometry (Table 2).

chloroplasts against photoinactivation under the very low CO_2 conditions of water stress is sometimes cited as a potentially useful function of photorespiration [3]. Grassy C_4 plants like corn and sugarcane suppress photorespiration by increasing leaf internal CO_2 concentrations [2], but this enrichment is an energy-expensive process. Soybeans and other C_3 plants use comparable energy to support nitrogen-fixing bacteria and live with photorespiration. The notion that a reduction in photorespiration in C_3 plants (induced either chemically or genetically) may translate into increased protein-rich crop yields is an idea that has been expressed frequently over the years [4,5].

1.2. Previous estimates of photorespiration

Optimistic reports (from the view of evolutionary success) claim that the rate of photorespiratory CO_2 loss is no more than 15% of the rate of net photosynthesis for well-fertilized leaves under ambient conditions [6], while less optimistic claims have set the rate as high as 50% [7]. The four conventional methods for measuring photorespiration in intact leaves are: (i) CO_2 efflux following abrupt darkness; (ii) enhancement of photosynthesis by low O_2; (iii) CO_2 efflux into CO_2-free air; and (iv) assimilation of label from $^{14}CO_2$. As noted by Sharkey [8], all four methods have technical problems, and this is the source of some of the ambiguity in the extent of photorespiration reported in the literature. The first is compromised by immediate dark respiration [9–11]; the second and third by the sensitivity of stomatal resistance (leaf gas-exchange rates) to an unusual atmosphere [12–14]; and the fourth by an unquantifiable dilution of administered ^{14}C by photorespired ^{12}C [15–17].

Because of these complications, stable-isotope strategies have been introduced recently in an effort to measure photorespiration more accurately. In one approach, $^{13}CO_2$ labeling distinguishes between CO_2 uptake and evolution under non-perturbing gas-exchange conditions. This is accomplished by mass spectrometric simultaneous detection of $^{13}CO_2$ and $^{12}CO_2$ in the gas flow around the leaf [18]. The labeling is done for short times (less than 30 s) and the evolved CO_2 is simply assumed to be totally unlabeled. The extent of re-assimilation of photorespired CO_2 must still be estimated from stomatal conductances and gas diffusion rates [18]. In a second stable-isotope approach, a measurement of net carbon assimilation by conventional gas-exchange methods is followed by a mass-spectrometric measurement of the ^{18}O enrichment of glycine [19], labeled by $^{18}O_2$ [20]. The glycine is extracted from the leaf, and the evolved CO_2 is calculated [19] based on the assumption that decarboxylation of glycine is a fixed proportion of oxygenation of Rubisco [8]. These stable-isotope measurements have been brought into agreement with gas-exchange estimates of photorespiration, (corrected using calculated stomatal conductances), as well as with predictions based on experimental in vitro kinetic parameters for Rubisco [8]. The consensus now reported in textbooks appears to be that in leaves of C_3 plants under ambient conditions, the rate of oxygenation to carboxylation of Rubisco is 0.4, and the rate of photorespiratory CO_2 release is about 25% of net CO_2 assimilation [21]. Both values are assumed to increase for low intercellular concentrations of CO_2 with a linear dependence on the external CO_2 concentration [8].

1.3. Photorespiration by NMR

In this paper, we report the direct measurement by NMR of photorespiration using in vivo labeling of soybean leaves with $^{13}CO_2$ (99 at.% ^{13}C, 200–400 ppm by volume in 21% O_2 and 79% N_2) for 2–8 min. The labeled leaf is removed from the plant, immediately frozen in liquid nitrogen and lyophilized. This procedure traps and preserves all labeled intermediates and products. Detection of all the label, soluble and insoluble, extractable and intractable is done by solid-state magic-angle spinning ^{13}C NMR of the intact, lyophilized leaf. No assumptions are made about gas exchange, gas re-assimilation, stomatal conduc-

tance, the decarboxylation rate of glycine, or the suitability of in vitro kinetics parameters to describe in vivo metabolism.

Two independent NMR measurements are made. In the first, changes in the transient ^{13}C isotopic enrichment of the phosphorylated Calvin-cycle intermediates are observed at fixed $^{13}CO_2$ labeling concentration, and these are related to the ratio of photosynthetic (p) to photorespiratory (r) carbon fluxes, p_c/r_c. The subscripts denote that the ratio of rates is measured by the isotopic enrichment of the Calvin cycle and so all the CO_2 that evolves results from glycerate production. The p_c/r_c ratio is the maximum possible value for the ratio of rates of photosynthesis and photorespiration. The ratio can be lowered by evolution of additional CO_2 from decarboxylation of glycine (produced in the light) that is not related to production of glycerate and maintenance of the Calvin cycle.

The ^{13}C isotopic enrichment of the Calvin cycle is determined by $^{13}C\{^{31}P\}$ rotational-echo double resonance (REDOR) NMR [22]. The sensitivity of REDOR to the internuclear separation of a heteronuclear pair of spins is used to determine the fraction of ^{13}C label in the leaf that is within two covalent bonds of ^{31}P. This is accomplished by using short carbon–phosphorous recoupling times (see Section 2), so that the REDOR difference spectrum detects only labeled phosphorylated carbons. This allows quantification of the ^{13}C isotopic enrichment of the Calvin cycle all of whose participants have a carbon that is two bonds from ^{31}P.

In the second solid-state NMR measurement, the net (or apparent) carbon assimilation is determined from a total ^{13}C-label spin count. The ^{13}C measurement is converted to net carbon (^{12}C plus ^{13}C) assimilation using the isotopic enrichment of the Calvin cycle known from the REDOR measurement. The apparent carbon assimilation rate differs from the photosynthetic rate because of photorespiration (*total* evolution of CO_2 in the light), and measurement of assimilation rates at two $^{13}CO_2$ concentrations therefore leads to a determination of p/r.

2. Materials and experimental methods

2.1. Growth of soybean plants

Glycine max (cv. Williams 82) was grown outdoors (June–August, 2004) on the roof of the Washington University McMillen Laboratories building. The soybeans were grown in 30-cm-diameter pots (6 plants per pot) filled with a mixture of one-third perlite and two-thirds top soil. Approximately 2 weeks after planting, when the first trifoliolates emerged, the pots were fertilized each day with 100 mL of a 1 g/L $^{15}NH_4{}^{15}NO_3$ solution. The ^{15}N label (99 at.% ^{15}N, Isotec, Miamisburg, OH) was used to distinguish ^{13}C label in amino acids from that in organic acids and proteins, analyses that will be described elsewhere. This high level of fertilizer suppressed symbiotic nitrogen fixation, as evidenced later by the scarcity of root nodules. The ^{15}N enrichment of the leaves was approximately 50%, as determined by solid-state ^{15}N NMR [23], less than that of the ammonium nitrate because of unlabeled nitrogen sources in the top soil. The plants were watered by hand, typically every 2 h during the day.

2.2. Labeling with $^{13}CO_2$

Labeling with $^{13}CO_2$ (99 at.% ^{13}C) was performed soon after flowers appeared, approximately 8 weeks after planting. The labeling was performed between 10 am and 2 pm on August 5, 2004, a bright sunny, cloud-free day with a temperature of 80 °F at noon in St. Louis. The windy conditions on the roof of the Chemistry Building resulted in soybean plants that were short (60 cm after 8 weeks) with thick stems and large leaves. The target central leaf of a trifoliolate (fifth or sixth node, uniform green coloration, typical surface area of 50 cm^2) was enclosed within a compact-disc jewel case (Fig. 2), which loosely fit around the stem and allowed the labeling gas to enter one end of the case, sweep over both surfaces of the leaf, and exit from the other end. The labeling was begun after confirmation of active photosynthesis by accumulation of moisture on the inner surface of the case. Gas mixtures in pressurized 6-L cylinders containing 21% O_2, 79% N_2, and the desired $^{13}CO_2$ concentration (199.8, 299.9, and 400.0 ppm by volume, Matheson Tri-Gas, Twinsburg, OH) flowed through this labeling chamber for specific time intervals (2–8 min). The gas flow was constant and was the equivalent of a turnover of 100 volumes of the labeling chamber per minute. This allowed a rapid complete exchange of $^{13}CO_2$ for $^{12}CO_2$ so that short labeling times were practical. An electric fan blew exiting gas away from the plants. No humidification of the labeling gas was attempted, but low CO_2 concentrations ensured open stomata and rapid gas exchange for the duration of the labeling [24,25]. Quantita-

Fig. 2. The $^{13}CO_2$ labeling of a soybean leaf using a compact-disc case as a labeling chamber. The labeling gas (21% O_2, either 200 or 300-ppm $^{13}CO_2$, and the balance N_2) entered at the bottom left through a copper pipe closed at the end and with multiple exit holes along the sides. At the end of the labeling period, the leaf was cut from its stem, immersed in liquid nitrogen, and subsequently lyophilized.

tive NMR analysis was performed only on leaves labeled with sub-ambient $^{13}CO_2$ concentrations. At the end of the labeling period, the leaf was cut from its stem and immersed in liquid nitrogen, a procedure that required less than 10 s. The frozen leaf was immediately lyophilized, after which 175 mg (of typically 225–250 mg) were chopped into approximately 1-mm fragments by hand with a razor blade, packed into a magic-angle spinning rotor, and examined by solid-state NMR. The petiole of the labeled leaf was not included with the chopped material but was examined separately.

2.3. Solid-state NMR

Spectra were obtained using a 6-frequency transmission-line probe [26], having a 12-mm long, 6-mm inside-diameter analytical coil and a Chemagnetics/Varian magic-angle spinning ceramic stator. Lyophilized samples were contained in thin-wall Chemagnetics/Varian 5-mm outside-diameter zirconia rotors. The rotors were spun at 7143 Hz with the speed under active control to within ±2 Hz. The spectrometer was controlled by a Tecmag pulse programmer. Radiofrequency pulses for ^{31}P (202 MHz), ^{13}C (125 MHz), and ^{15}N (50.3 MHz) were produced by 1-kW American Microwave Technology power amplifiers. Proton (500 MHz) radiofrequency pulses were generated by a 1-kW Amplifier Systems tube amplifiers driven by a 50-W American Microwave Technology power amplifier. The π-pulse lengths were 6 μs for ^{31}P, 8 μs for ^{13}C, and 9 μs for ^{15}N. A 12-T static magnetic field was provided by an 89-mm bore Magnex superconducting solenoid. Proton-carbon cross-polarization magic-angle spinning (CPMAS) transfers were made with radiofrequency fields of 62.5 kHz. Proton dipolar decoupling was 100 kHz during data acquisition.

REDOR was used to restore the dipolar couplings between heteronuclear pairs of spins that are removed by magic-angle spinning [22]. REDOR experiments are always done in two parts, once with rotor-synchronized dephasing pulses (S) and once without (full echo, S_0). The dephasing pulses change the sign of the heteronuclear dipolar coupling, and this interferes with the spatial averaging resulting from the motion of the rotor. The difference in signal intensity (REDOR difference, $\Delta S = S_0 - S$) for the observed spin in the two parts of the REDOR experiment is directly related to the corresponding distance to the dephasing spin [22]. REDOR has found application in the characterization of binding sites of proteins [27], and in the analysis of heterogeneous biological materials such as amyloid plaques [28], membrane protein helical bundles [29], and bacterial cell walls [30]. All $^{13}C\{^{31}P\}$ REDOR spectra were collected with standard xy-8 phase cycling [31], on both observed and dephasing channels.

3. Results

3.1. Photorespiration from the transient isotopic enrichment of the Calvin cycle

The full-echo ^{13}C NMR spectrum of a soybean leaf labeled for 2 min by 300-ppm $^{13}CO_2$ has resonances characteristic of the major protein and sugar components (Fig. 3, bottom left). The protein peaks have the same intensities as those of a leaf at natural abundance (not shown), and the sugar peak is slightly enhanced. The 8-rotor cycle $^{13}C\{^{31}P\}$ REDOR difference spectrum, on the other hand, has a significant intensity for the sugar peak, more than five times that of an unlabeled leaf (Fig. 3, upper left). These spectra indicate that by 2 min after the start of labeling, gas exchange has replaced unlabeled CO_2 within the leaf and the Calvin cycle intermediates are already at least partially labeled.

The $^{13}C\{^{31}P\}$ REDOR differences in Fig. 3 are referenced to the integrated intensity of all of the natural-abundance aliphatic-carbon protein peaks between 0 and

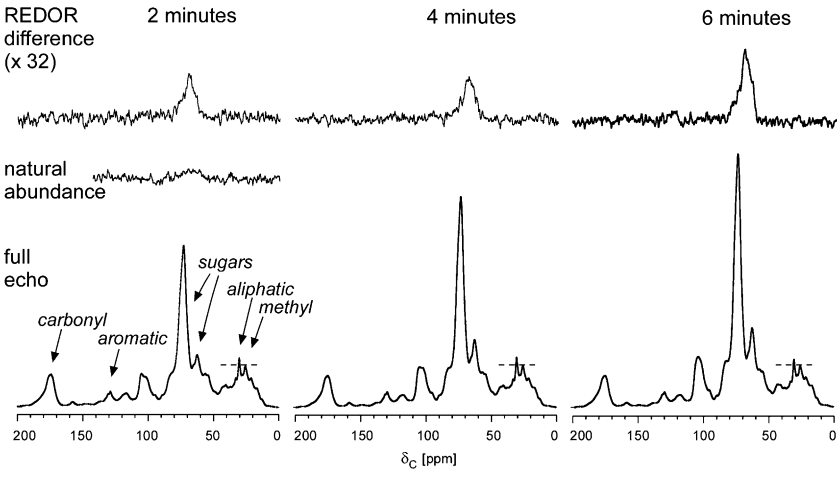

Fig. 3. $^{13}C\{^{31}P\}$ eight rotor-cycle rotational-echo double-resonance (REDOR) spectra of soybean leaves labeled by 300-ppm (by volume) $^{13}CO_2$ for 2–6 min. The REDOR difference spectra ($S_0 - S$) are at the top of the figure and the full-echo spectra (S_0) at the bottom. The full-echo spectra have been normalized by their natural-abundance methyl-carbon peaks (dotted lines). The REDOR difference arises from Calvin-cycle intermediates with ^{13}C-labeled phosphorylated carbons. Each spectrum resulted from the accumulation of 50,000 scans. Magic angle spinning was at 7143 Hz.

30 ppm, which have been normalized to one another, thereby minimizing the effect of possible differences in protein content between leaves. The normalization means that the REDOR difference intensity is referenced to the Rubisco concentration, assuming the same protein composition from leaf to leaf.

By 4 min after the start of labeling, the accumulation of ^{13}C in the full-echo sugar peak is obvious (Fig. 3, bottom middle). The major sugar peak has a shift of 72.6 ppm (relative to external [1-^{13}C]glycine at 179 ppm). However, the $^{13}C\{^{31}P\}$ REDOR difference peak has not significantly increased (Fig. 3, top middle). This result indicates that as soon as 2 min after the start of labeling, all $^{12}CO_2$ within the leaf had been replaced by $^{13}CO_2$, and ^{13}C label had been distributed uniformly within RuBP. However, the ^{13}C isotopic enrichment of RuBP is not 99%, but a lower value that depends on the flux of salvaged photorespiratory *unlabeled* carbon returned to the Calvin cycle as (phospho)glycerate (Fig. 1). This situation persists for 4 min of labeling. Because any CO_2 produced by glycine decarboxylation in the mitochondria (see Fig. 1) between 2 and 4 min is labeled at the same enrichment as that of RuBP itself, this carbon source has a secondary effect on the isotopic enrichment of the Calvin cycle. If the photorespired CO_2 escapes the leaf, it has no effect on the labeling because of the rapid gas turnover in the labeling chamber (see Section 2). The dilution of the Calvin cycle is therefore dominated by the recycled glycerate, which for at least 4 min after the first application of $^{13}CO_2$ is totally unlabeled (Table 1).

Table 1
Isotopic enrichment of the Calvin cycle (f_k^m) during $^{13}CO_2$ labeling of soybean leaves[a]

CO_2 concentration (k) [ppm]	Labeling period (m) [min]	f_k^m
200	2	0.63
	4	0.62
	6	1.03
	8	0.97
300	2	0.63
	4	0.66
	6	1.00[b]
	8	0.95

[a] From 8-T_r $^{13}C\{^{31}P\}$ REDOR ΔS, with S_0 scaled by comparison to natural-abundance protein peaks (0–30 ppm); f_k^m values are ΔS areas relative to the ΔS area for 300-ppm $^{13}CO_2$ labeling for 6 min.
[b] Reference enrichment (arbitrary).

For 6 min of labeling, the full-echo sugar-peak continues to accumulate intensity at the rate established by 4 min (Fig. 3, bottom right). This approximately linear response indicates no substantive change in internal temperature or stomatal conductance of the leaves resulting from the labeling conditions. Despite the uniform accumulation of label between 4 and 6 min, the REDOR difference peak jumps in intensity by 60% (Fig. 3, top right), and then remains at this higher level for the longest labeling time of 8 min (Table 1). This jump in intensity indicates the arrival in the chloroplasts of labeled glycerate from the photorespiratory pathway. The corresponding $^{13}C\{^{31}P\}$ REDOR results for labeling with 200-ppm $^{13}CO_2$ indicate a similar delay after the start of labeling before the arrival of labeled glycerate, and a similar jump in isotopic enrichment of the Calvin cycle (Table 1).

The stoichiometry of the Calvin cycle is summarized in Table 2 for a fixed number of Rubisco sites, but with variations in carboxylase/oxygenase activity under standard atmospheric conditions. The resulting relative carbon fluxes are determined by reference to Fig. 1 (see parenthetical numbers). We designate the expected isotopic enrichment of the Calvin cycle after reaching a steady-state labeling of the chloroplasts, but *before* labeling of glycerate returning from the peroxisomes as f^{initial}, and the expected enrichment after labeling of the glycerate as f^{final} (Table 2).

To determine the ratio of the rate of photosynthesis to the rate of photorespiration (p_c/r_c), we take f^{initial} as the observed isotopic enrichment between 2 and 4 min after the start of labeling, and f^{final} as the observed enrichment between 6 and 8 min. (In preliminary soybean labeling experiments performed over the summers of 2001–2003, we labeled with 200 ppm $^{13}CO_2$ for times as long as 20 min and observed that the isotopic enrichments did not increase further and were comparable to the 6 and 8-min values of Table 1.) The experimentally observed $f^{\text{initial}}/f^{\text{final}}$ ratio is 0.64 for 300-ppm $^{13}CO_2$ labeling, and 0.63 for 200-ppm labeling (Table 1), with a leaf-to-leaf variability of about 5%. These values indicate a p_c/r_c of 5.7 (Fig. 4) for both labeling concentrations.

3.2. Net carbon assimilation rates

The apparent photosynthetic rate (A) is diminished from the true photosynthetic rate (p) by the rate at which CO_2 is

Table 2
Stoichiometry of the Calvin cycle under normal atmospheric conditions in the presence of photorespiration[a]

CO_2 in	O_2 in	Glycerate carbons in	CO_2 out	Triose-P cycled	–(CH_2O)– stored	$f^{\text{initial}}/f^{\text{final}}$ [b]	p/r[c]
8	2	3	1	19	7	8/11 (0.727)	8
6	4	6	2	18	4	6/12 (0.500)	3
4	6	9	3	17	1	4/13 (0.308)	1.33
0	10	—	10	—	0	0	0

[a] From Fig. 1.
[b] From the ratio of entries in column 1 to the sum of those in columns 1 and 3.
[c] From the ratio of entries in columns 1 and 4.

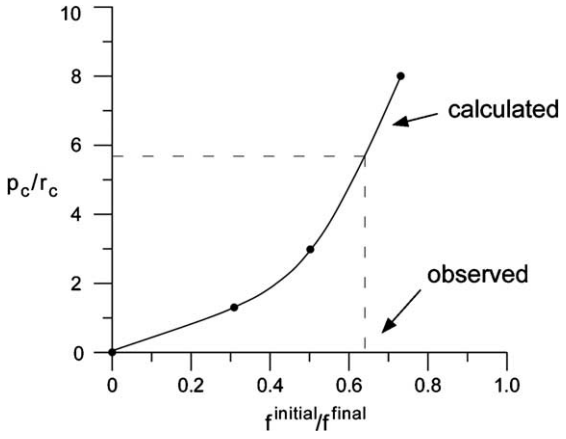

Fig. 4. The expected ratio of photosynthesis (p) to photorespiration (r) as a function of the isotopic enrichment of the Calvin cycle in a $^{13}CO_2$ labeling experiment before ($f^{initial}$) and after (f^{final}) the appearance in the chloroplasts of ^{13}C-labeled glycerate from the photorespiratory pathway. The solid circles are the calculated values in Table 2; the solid line is a polynominal fit. (Middle) Schematic representation of carbon flux in the Calvin cycle and the photorespiratory C_2 cycle under near-ambient conditions. The thickness of any section of the cycle is proportional to the associated rate.

generated by photorespiration (r) so that under standard atmospheric conditions in the light,

$$A = p - r. \quad (1)$$

This expression assumes that there is no significant dark respiration [32]. To obtain the total carbon-assimilation rate (A_k^m) for period (m) and $^{13}CO_2$ labeling concentration (k), the experimentally observed ^{13}C assimilation rate (C_k^m) is scaled by the ^{13}C isotopic enrichment (f_k^m) of the Calvin cycle so that:

$$A_k^m = C_k^m / f_k^m. \quad (2)$$

The f_k^m are the REDOR-determined isotopic enrichments of the Calvin cycle discussed above (Fig. 3 and Table 1) and the C_k^m are determined from *differences* of cross-polarization magic-angle spinning (CPMAS) ^{13}C NMR measurements.

In solid-state ^{13}C NMR, the most accurate ^{13}C signal intensities are obtained by a systematic variation of the length of the CPMAS matched proton-carbon spin–lock contact [33]. This sort of procedure (with variation of contact time from 0.2 to 12.0 ms) results in relative signal intensities that are independent of all rotating-frame relaxation parameters. These CPMAS intensities are then compared leaf-to-leaf on an absolute basis by normalization with respect to the natural-abundance aliphatic-carbon signal intensities between 0 and 30 ppm. The normalization reduces the effect of variations in protein content between leaves. Examples of normalized CPMAS spectra obtained in experiments performed on leaves labeled for 2–6 min with either 200 or 300 ppm $^{13}CO_2$ are shown in Fig. 5. The 75-ppm signal intensity, highlighted by a dotted line in all six spectra, increases uniformly with time and faster at higher $^{13}CO_2$ labeling concentration, a combination that clearly indicates the accumulation of label.

Signals from just the ^{13}C label after labeling for 2 min are obtained by subtracting the spectrum of a lyophilized leaf at natural abundance (Fig. 6). The sugar peaks are dominant but significant label also accumulates in methylene carbons (42 ppm) and carbonyl-carbons of glycine (179 ppm) and, at sub-ambient CO_2 labeling concentrations, glycyl residues in protein (171 ppm). The latter assignments have been made using $^{13}C\{^{15}N\}$ REDOR (see Fig. 1 in [34]).

For 400-ppm $^{13}CO_2$, almost all of the carbonyl-carbon peak is due to glycine (Fig. 6, inset). This is consistent with all of the products of the oxygenase activity of Rubisco

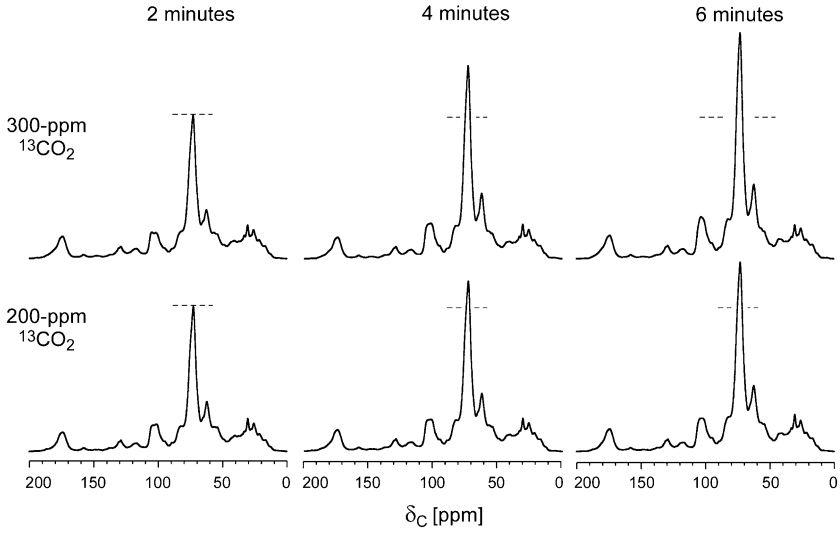

Fig. 5. Cross-polarization magic-angle ^{13}C NMR spectra of intact lyophilized soybean leaves labeled for 2, 4, or 6 min with $^{13}CO_2$ at 200 ppm (bottom) or 300 ppm (top), both concentrations by volume. The 62.5-kHz matched spin–lock contact time was 1 ms. Each spectrum resulted from the accumulation of 20,000 scans. The accumulation of label (dotted lines) is approximately linear between 2 and 6 min at both labeling concentrations. These spectra were used in the determination of the carbon assimilation rates of Table 3.

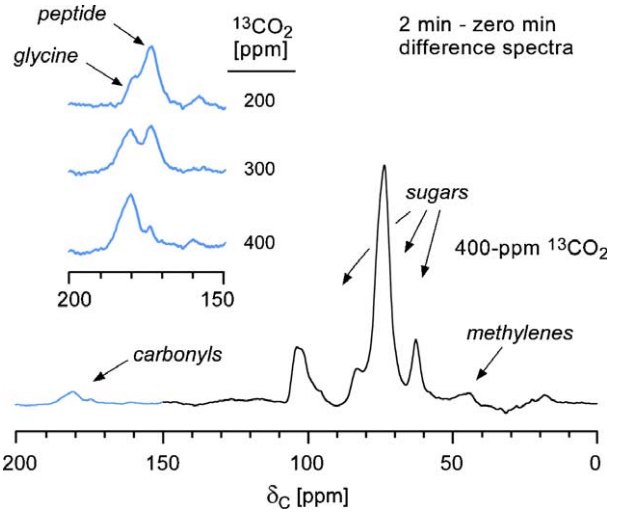

Fig. 6. Cross-polarization magic-angle ^{13}C NMR spectrum of label accumulated by a soybean leaf labeled for 2 min with $^{13}CO_2$ at 400 ppm (by volume), and compared with leaves labeled with $^{13}CO_2$ at 300 and 200 ppm (inset). These are difference spectra resulting from the subtraction of the spectrum of an unlabeled leaf. Each of the spectra of the differences resulted from the accumulation of 130,000 scans. The inset (in blue) shows that the distribution of label between the 171- and 179-ppm carbonyl-carbon peaks changes as a function of the concentration of $^{13}CO_2$ used for labeling.

entering the C_2 cycle and returning to the Calvin cycle as glycerate (Fig. 1). Thus, for every 8 oxygenations of Rubisco, there are 4 decarboxylations of glycine ultimately resulting in 4 glycerates. For 300-ppm $^{13}CO_2$ labeling however, the relative intensities of the carbonyl-carbon peaks (Fig. 6, inset) are 3:2 (glycine:peptide). This is the ratio expected if glycerate production is reduced by 1/4 (to match the reduced activity of the Calvin cycle) and the excess 2 glycines are both saved in protein. This means that the total CO_2 released by photorespiration is *reduced* by 25% and for every two oxygenations of Rubisco there is *less* than one decarboxylation. For 200-ppm $^{13}CO_2$ labeling on the other hand, the glycine:peptide ratio is about 1:4 rather than the expected 2:4 if photorespired CO_2 were reduced by an additional 25%. Thus, some of the excess glycine for these labeling conditions has been decarboxylated. We will return to this point later in the next section when we develop equations to describe p/r by total carbon assimilation quantitatively.

The CPMAS signal intensity (integrated over the entire spectrum) for the leaf labeled with 300 ppm $^{13}CO_2$ for 4 min, minus that for the leaf labeled for 2 min, translates into an increase of 0.242 μg ^{13}C per milligram of leaf per minute at 300 ppm. This is the ^{13}C assimilation rate, C_{300}^{4-2} (Table 3). Using the commonly reported units per square meter of leaf area per second, the ^{13}C assimilation rate is 17 μmol $^{13}C\ m^{-2}\ s^{-1}$. All the ^{13}C assimilation rates determined in the CPMAS experiments of Fig. 5 are reported in Table 3, along with the total carbon assimilation rates determined from $A_k^m = C_k^m/f_k^m$ and the f_k^m of Table 1. To determine A_k^{4-2}, we note that f_k^2 and f_k^4 are almost equal and so we use their average (0.64) for f_k^{4-2}. If we also use a simple arithmetic average for the isotopic enrichment appropriate for the $6-4$ min difference of labeling times, that is, $f_k^{6-4} = (f_k^4 + f_k^6)/2 = 0.82$, then we find A_k^{6-4} values that are slightly less than the corresponding A_k^{4-2} values (Table 3). This result suggests that f_k^{6-4} should be less than 0.82, which means that the arrival of [^{13}C]glycerate was a little later than 5 min after the start of labeling. Because a 6-min labeling time is short enough that there is no ^{13}C export from the leaf [35] (no label was detected in detached petioles even after 8 min of leaf labeling), the CPMAS difference experiment provides a complete accounting of assimilated carbon label in the leaf. Rotor-synchronized Hahn-echo experiments using 90° ^{13}C inspection pulses confirmed that there was no label in the more liquid-like components of the lyophilized leaf tissue [36].

3.3. Photorespiration by carbon assimilation rates

Between 200 and 400 ppm, p is a linear function of (external) CO_2 concentration [37]. Thus, if we take 400 ppm as the ambient concentration (a), we have

$$A_{300}^m = p_{300} - r_{300} = 3p_a/4 - 3r_a/4 = C_{300}^m/f_{300}^m, \quad (3)$$

$$A_{200}^m = p_{200} - r_{200} = p_a/2 - x/2 = C_{200}^m/f_{200}^m, \quad (4)$$

where p_a and r_a are rates at 400-ppm CO_2, and $x/2$ is the rate of photorespiration at 200-ppm CO_2. The 3/4 coefficient for the r_a term in Eq. (3) reflects the reduction of photorespired CO_2 shown in Fig. 6 (inset, middle) and discussed in the previous section. We take the extent of released CO_2 for 200-ppm labeling as an unknown. If $x/2 = r_a/2$, all excess glycine is saved in protein; if $x/2 = r_a$,

Table 3
Carbon assimilation rates (A_k^m) and ^{13}C assimilation rates (C_k^m) for soybean leaves labeled with $^{13}CO_2$.

$^{13}CO_2$ concentration (k) [ppm]	Time interval difference (m) [min]	Total NMR ^{13}C label[a] [μg]	C_k^m [μg $^{13}C\ mg^{-1}\ min^{-1}$][b,c]	A_k^m [μg $C\ mg^{-1}\ min^{-1}$][b]
200	4 – 2	48.4	0.138	0.216
	6 – 4	56.4	0.161	0.196
300	4 – 2	84.6	0.242	0.378
	6 – 4	96.3	0.275	0.335

[a] Calibrated by a natural-abundance CPMAS ^{13}C NMR spectrum of a lyophilized leaf.
[b] Units are expressed in mg of lyophilized leaf tissue.
[c] Estimated accuracy is ±0.005 based on signal-to-noise ratios.

Table 4
Comparisons of rates of photosynthesis (p) and photorespiration (r) as determined by gas exchange/rubisco kinetics and NMR

Method, CO_2 concentration (ppm)	CO_2 in	O_2 in	V_O/V_C[a]	CO_2 out	–CH_2O– saved	p/r	r/–CH_2O–[b]
Gas exchange, 400	6.25	2.5[c]	.40[d]	1.25	5.0	5.0	.25[d]
300	4.7	2.5	.53	1.25	3.4	3.8	.37
200	3.2	2.5	.80	1.25	1.9	2.5	.66
NMR, 400	5.7	2.0	.35	1	4.7	5.7[e]	.21
300	4.3	2.0	.47	.75[f]	3.6	5.7[f]	.21
200	3.5	2.0	.70	1	2.5	3.5[g]	.40

[a] Ratio of oxygenase activity to carboxylase activity for Rubisco.
[b] Rate of photorespiratory release to rate of net CO_2 assimilation.
[c] By assumption: two oxygenations of Rubisco for every CO_2 release under ambient external CO_2.
[d] From Ref. [8].
[e] Projected from isotopic-dilution values of p_c/r_c at 200 and 300-ppm CO_2 concentrations (Fig. 4), and results of Fig. 6 (see text).
[f] From Fig. 6 (see text).
[g] From Eq. (5) and Table 3.

the rate of decarboxylation is the same as under normal ambient conditions; if $x/2 > r_a$, then less carbon is salvaged than under normal ambient conditions.

The two expressions for apparent photosynthetic rates as a function of $^{13}CO_2$ concentration are combined to determine the ratio of the photosynthetic and photorespiratory rates (at 200-ppm CO_2), which is

$$p_{200}/r_{200} = p_a/x = 1/\{1 - 3R(1 - r_a/p_a)/2\}, \quad (5)$$

where $R = f^m_{300}C^m_{200}/f^m_{200}C^m_{300}$. For the 4 −2 min labeling interval, the f_k^{4-2} cancel (Table 1) and $R = 0.57$ (.138/.242, Table 3) and $p_a/x = p_{200}/r_{200} = 3.4$. The f_k^{6-4} also cancel in the $6 - 4$ min labeling interval ($f^{6-4}_{200} = .825$ and $f^{6-4}_{300} = .830$), $R = 0.59$ and $p_a/x = 3.7$. The average is 3.5 (Table 4) which corresponds to using a $6 - 2$ min labeling interval. Because p_a/x (and in general, p/r at any concentration) is determined from A's, which are *ratios* of f's and C's, there is no (^{13}C vs. ^{12}C) kinetic isotope effect.

4. Discussion

4.1. Photorespiration at sub-ambient CO_2 concentrations

The similarity of p_c/r_c values for 200 and 300-ppm $^{13}CO_2$ labeling determined by $^{13}C\{^{31}P\}$ REDOR indicates that in vivo Rubisco is not kinetically modified in response to decreasing CO_2 concentrations. The Calvin cycle simply turns over more slowly at the lower CO_2 levels (Fig. 7). The amount of glycerate from the C_2 cycle entering the Calvin cycle therefore does not remain constant (or increase) at low CO_2 concentration, but rather decreases, which means that the photorespiratory release of CO_2 resulting from glycerate production (via glycine and serine) also decreases. If excess glycine from the C_2 cycle (i.e., glycine not used for the production of glycerate) is subsequently decarboxylated [38], this release of CO_2 does not indicate a lowered value of the ratio of photosynthesis to photorespiration in the sense of the carboxylase/oxygenase ratios of Table 2, but rather the activity of other metabolic processes in the leaf [34,39].

4.2. Comparisons of NMR and gas-exchange determinations of photorespiration

The determination of $p_c/r_c \approx 6$ at sub-ambient CO_2 concentrations (Fig. 4) shows that the rate of CO_2 release as part of glycerate production decreases as the photosynthetic rate decreases. Estimates of CO_2 release based either totally or partially on gas-exchange measurements or kinetics calculations, on the other hand, generally maintain that the rate of CO_2 release is unchanged under low CO_2 conditions [8]. However, such estimates do not take into account

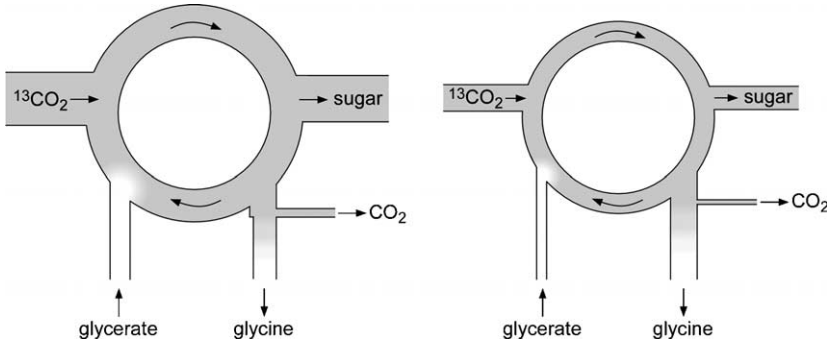

Fig. 7. At reduced external CO_2, the relative rates of flow of ^{13}C (shaded) and ^{12}C (white) into the Calvin cycle are unchanged. The ratio of photosynthetic CO_2 (in) to photorespiratory CO_2 (out) is also unchanged, but the flow of carbon into glycine has increased. Part of this glycine is converted into glycerate, while the remainder may be incorporated into other products, or, depending on the metabolic state of the leaf, decarboxylated.

the multiple metabolic routes for the processing of excess glycine, which include full decarboxylation, partial decarboxylation (for glycerate production), and no decarboxylation (for protein synthesis). Thus, for every two oxygenations, there may be less than one or more than one CO_2 released (see Table 4), a variability which appears to depend on the status of the nitrogen metabolic pools [34]. For example, as described above and illustrated in Fig. 6, the leaf labeling at 300-ppm $^{13}CO_2$ did not involve decarboxylation of excess glycine while the leaf labeling at 200-ppm $^{13}CO_2$ did. A value of one CO_2 released is consistent with both gas-exchange and NMR estimates of photorespiration under near-ambient conditions (Table 4), and with the observation that little of the glycine resulting from oxygenation of Rubisco is diverted from the C_2 pathway under near-ambient conditions (Fig. 6). However, at sub-ambient CO_2 concentrations, less CO_2 is released than anticipated and the NMR-determined values for p/r are substantially greater than the corresponding gas-exchange values (Table 4).

Based on the previous discussion, we believe that in vivo $^{13}CO_2$ labeling with solid-state NMR detection of label makes two substantive advances in the measurement of photorespiration in leaves: (i) the NMR method is direct and requires no supplementary measurements or calculations of leaf physical or kinetics parameters; and (ii) the NMR method determines the extent to which glycine resulting from the oxygenation of Rubisco is diverted from the C_2 pathway and so avoids assumptions about the rate of decarboxylation of glycine.

4.3. Photorespiration assays in the field

The method we have used to determine photorespiration in the leaves of soybeans grown in pots is easily extended to other plants and growing conditions. The labeling apparatus is simple, portable, requires no elaborate calibration, and can be used in awkward locations like tree tops [40]. The labeling times are short and release of the label in the environment is harmless. The necessary NMR analysis (including REDOR) is now standard on a modern solids spectrometer, equipped with a 3-frequency high-power probe, and can be performed at any time that is convenient after the labeling. With the sensitivity and reliability of the REDOR analysis, we believe that it should be possible to establish unambiguously whether photorespiration (i.e., total CO_2 released in the light) varies from one C_3 plant species to another. The answer to this question could help in deciding whether the transformation of crop plants with foreign Rubisco to enhance net CO_2 assimilation would indeed result in increased productivity [41]. In addition, it should be possible to establish whether photorespiration varies from one set of metabolic conditions to another in the same species. The answer to this question may point to a short-term function for photorespiration [34] that is complementary to its apparent long-term support of nitrate assimilation [39].

References

[1] E. Broda, The Evolution of Bioenergetic Processes, Pergamon, Oxford, 1975.
[2] R. Douce, H.W. Heldt, Photorespiration, Adv. Photosyn. 9 (2000) 115–136.
[3] R. Douce, M. Neuburger, Biochemical dissection of photorespiration, Curr. Opin. Plant Bio. 2 (1999) 214–222.
[4] I. Zelitch, Increased rate of net photosynthetic carbon dioxide uptake caused by the inhibition of glycolate oxidase, Plant Physiol. 41 (1996) 1623–1631.
[5] X.-G. Zhu, A.R. Portis Jr., S.P. Long, Would transformation of C_3 crop plants with foreign Rubisco increase productivity? A computational analysis extrapolating from kinetic properties to canopy photosynthesis, Plant Cell Environ. 27 (2004) 155–165.
[6] W.L. Ogren, Photorespiration: pathways, regulation, and modification, Ann. Rev. Plant Physiol. 35 (1984) 415–442.
[7] I. Zelitch, Pathways of carbon fixation in green plants, Ann. Rev. Biochem. 44 (1975) 123–145.
[8] T.D. Sharkey, Estimating the rate of photosynthesis in leaves, Physiol. Plant 73 (1988) 147–152.
[9] J. Azcon-Bieto, C.B. Osmond, Relationship between photosynthesis and photorespiration. The effect of carbohydrate status on the rate of CO_2 production by respiration in darkened and illuminated wheat leaves, Plant Physiol. 71 (1983) 574–581.
[10] A. Laisk, O. Kiirats, V. Oja, Assimilatory power (post illumination CO_2 uptake) in leaves, Plant Physiol. 35 (1984) 415–422.
[11] T.D. Sharkey, J.R. Seemann, R.W. Percy, Contribution of metabolites of photosynthesis to post illumination CO2 assimilation in response to lightflecks, Plant Physiol. 82 (1986) 1063–1068.
[12] T.D. Sharkey, O_2-insensitive photosynthesis in C_3 plants. Its occurrence and a possible explanation, Plant Physiol. 78 (1985) 71–75.
[13] M.R. Badger, T.D. Sharkey, S. von Caemmerer, The relationship between steady-state gas exchange of bean leaves and the levels of carbon-reduction-cycle intermediates, Planta 160 (1984) 305–313.
[14] S. von Caemmerer, D.L. Edmondson, The relationship between steady-state gas exchange, in vivo RuP2 carboxylase activity and some carbon reduction cycle intermediates in *Raphanus sativus*, Aust. J. Plant Physiol. 13 (1986) 669–688.
[15] A. Gerbaud, M. Andre, An evaluation of the recycling in measurements of photorespiration, Plant Physiol. 83 (1987) 933–937.
[16] G.D. Farquhar, M.H. O'Leary, J.A. Berry, On the relationship between carbon isotope discrimination and the intercellular carbon dioxide concentration in leaves, Aust. Plant J. Physiol. 9 (1982) 121–137.
[17] M.H. O'Leary, Carbon isotope fractionation in plants, Phytochemistry 20 (1981) 553–567.
[18] S. Haupt-Herting, K. Klug, H.P. Fock, A new approach to measure gross CO_2 fluxes in leaves. Gross CO_2 assimilation, photorespiration, and mitochondrial respiration in the light in tomato under drought stress, Plant Physiol. 126 (2001) 388–396.
[19] E.J. de Veau, J.E. Buris, Photorespiratory rates in wheat and maize as determined by ^{18}O-labeling, Plant Physiol. 90 (1989) 500–511.
[20] S. Haupt-Herting, H.P. Fock, Exchange of oxygen and its role in energy dissipation during drought stress in tomato plants, Physiol. Plant 110 (2000) 489–495.
[21] B.B. Buchanan, W. Gruissem, R.L. Jones, Biochemistry and Molecular Biology of Plants, American Society of Plant Physiologists, Rockville, MD, 2000, p. 725.
[22] T. Gullion, J. Schaefer, Detection of weak heteronuclear dipolar coupling by rotational-echo double-resonance NMR, Adv. Magn. Reson. 13 (1989) 58–83.
[23] J. Schaefer, E.O. Stejskal, R.A. McKay, Cross-polarization of N-15 labeled soybeans, Biochem. Biophys. Res. Commun. 88 (1979) 274–280.
[24] J.A. Bunce, Effects of humidity on short-term responses of stomatal conductance to an increase in carbon dioxide concentration, Plant, Cell Environ. 21 (1998) 115–120.

[25] S. von Caemmerer, T. Lawson, K. Oxborough, N. Baker, T.J. Andrews, C.A. Raines, Stomatal conductance does not correlate with photosynthetic capacity in transgenic tobacco with reduced amounts of Rubisco, J. Exp. Bot. 55 (2004) 1157–1166.

[26] J. Schaefer, R.A. McKay, Multi-tuned single coil transmission line probe for nuclear magnetic resonance spectrometer, U.S. Patent 5,861,748 (1999).

[27] L.M. McDowell, B. Poliks, D.R. Studelska, R.D. O'Connor, D.D. Beusen, J. Schaefer, Rotational-echo double-resonance NMR-restrained model of the ternary complex of 5-enolpyruvylshikimate-3-phosphate synthase, J. Biomol. NMR 28 (2004) 11–29.

[28] J.J. Balbach, Y. Ishii, O.N. Antzutkin, R.D. Leapman, N.W. Rizzo, F. Dyda, J. Reed, R. Tycko, Amyloid fibril formation by A β16–22, a seven-residue fragment of the Alzheimer's β-amyloid peptide and structural characterization by solid state NMR, Biochemistry 39 (2000) 13748–13759.

[29] S.O. Smith, T. Kawakami, W. Liu, M. Zilios, S. Aimoto, S. Helical, structure of phospholamban in membrane bilayers, J. Mol. Biol. 313 (2001) 1139–1148.

[30] L. Cegelski, S.J. Kim, A.H. Hing, D.R. Studelska, R.D. O'Connor, A.K. Mehta, J. Schaefer, Rotational-echo double-resonance characterization of the effects of vancomycin on cell wall synthesis in *Staphylococcus aureus*, Biochemistry 41 (2002) 13053–13058.

[31] T. Gullion, D.B. Baker, M.S. Conradi, New, compensated Carr—Purcell sequences, J. Magn. Reson. 89 (1990) 479–484.

[32] T. Parnik, O. Keerberg, Decarboxylation of primary and end products of photosynthesis at different oxygen concentrations, J. Exp. Bot. 46 (1995) 1439–1447.

[33] E.O. Stejskal, J. Schaefer, T.R. Steger, High resolution ^{13}C nuclear magnetic resonance in solids, Far. Symp. Chem. Soc. 13 (1978) 56–62.

[34] L. Cegelski, J. Schaefer, Glycine metabolism in intact leaves by in vivo ^{13}C and ^{15}N labeling, J. Biol. Chem. 280 (2005) 39238–39245.

[35] M.R. Thorpe, K.B. Walsh, P.E.H. Minchin, Photoassimilate partitioning in nodulated soybean I. ^{11}C methodology, J. Exp. Bot. 49 (1998) 1805–1815.

[36] J.R. Garbow, J. Schaefer, Magic-angle $_{13}C$ NMR study of what flours and doughs, J. Agric. Food Chem. 19 (1991) 877–880.

[37] S. von Caemmerer, J.R. Evans, G.S. Judson, T.J. Andrews, The kinetics of ribulose bisphosphate carboxylase-oxygenase in vivo inferred from measurements of photosynthesis in leaves of transgenic tobacco, Planta 195 (1994) 88–97.

[38] R. Douce, J. Bourguignon, M. Neuburger, F. Rébeillé, The glycine decarboxylase system: a fascinating complex, Trends Plant Sci. 4 (2001) 167–176.

[39] S. Rachmilevitch, A.B. Cousins, A.J. Bloom, Nitrate assimilation in plant shoots depends on photorespiration, Proc. Natl. Acad. Sci. USA 101 (2004) 11506–11510.

[40] I.J. Wright, P.B. Relch, M. Westoby, D.D. Ackerly, Z. Baruch, F. Bongers, J. Cavender-Bares, T. Chapin, J.H.C. Cornellssen, M. Diemer, J. Flexas, E. Garnier, P.K. Groom, J. Gullas, K. Kikosaka, B.B. Lamont, T. Lee, W. Lee, C. Lusk, J.J. Midgley, M.-L. Manas, U. Nilnemets, J. Oleksyn, N. Osada, H. Poorter, P. Poot, L. Prior, V.I. Pyankov, C.A. Roumet, S.C. Thomas, M.G. Tjoelker, E.J. Veneklaas, R. Pillar, The worldwide leaf economics spectrum, Nature 428 (2004) 821–827.

[41] R.J. Spreitzer, M.E. Salvucci, Rubisco: structure, regulatory interactions, and possibilities for a better enzyme, Annu. Rev. Plant Biol. 53 (2002) 449–475.